

Cermet compact made from semiconducting InSb with constant electrical resistance in the 4–400 K range

M. JERSEL, J. ČERVENÁK, V. ŠMATKO, V. ŠTRBÍK

Institute of Electrical Engineering, Slovak Academy of Sciences, SK-842 39 Bratislava, Slovakia

F. HANIC, M. KUBRANOVÁ

Institute of Inorganic Chemistry, Slovak Academy of Sciences, SK-842 36 Bratislava, Slovakia

I. TRAVĚNEC, V. KLIMENT

Institute of Physics, Slovak Academy of Sciences, SK-842 28 Bratislava, Slovakia

A study of the electrophysical properties of samples prepared by phase transformation of stoichiometric InSb into InSb–Sb–In₂O₃ cermet compact has been performed (InSb, In₂O₃-semiconductors, antimony-metallic conductivity). Samples were prepared by isothermal partial oxidation at 200–500 °C for 1–50 h. Bulk and thin-film samples annealed at 400 °C for 1–50 h possess relatively constant electrical resistance over the wide temperature interval measured: 4–400 K. The conversion degree, β , and molar ratio, $f = \text{In}_2\text{O}_3/2\text{Sb}$ were calculated from the isothermal thermogravimetry data according to the reaction equation $2\text{InSb} + 3/2\text{O}_2 = \text{In}_2\text{O}_3 + 2\text{Sb}$ at temperatures $T < 400$ °C, when no ascertainable amount of antimony is escaping from the system. The β -value increases with temperature, T , and time of oxidation annealing, t . However, instead of being constant, i.e. $f = 0.5$, f increases for $T > 400$ °C and $t > 1$ h. The X-ray powder diffraction, thermogravimetry, differential thermogravimetry and differential thermal analysis measurements and studies revealed that metallic antimony escapes partially from the InSb–Sb–In₂O₃ system obtained at $T \geq 400$ °C. As a result, the mutual volume ratio of individual InSb, Sb and In₂O₃ components is changed, and so also is the overall character of the electrical resistivity of the samples. Due to the partial escape of Sb↑ from the system at $T \geq 400$ °C, the following reaction is appropriate: $2\text{InSb} + 3/2\text{O}_2 = \text{In}_2\text{O}_3 + (2 - z)\text{Sb}\uparrow = \text{In}_2\text{O}_3 + \text{Sb}/f + z\text{Sb}$, where z is the volatilized portion of Sb and f is the molar ratio of the reaction products, i.e. $f = \text{In}_2\text{O}_3/(2 - z)\text{Sb} = 1/(2 - z)$. The SEM observations revealed a growing grain size with temperature and time of annealing, lowering the grain-boundary density and thus also the resistivity of the samples. The properties of the obtained ternary compact may be influenced significantly, if instead of stoichiometric InSb, the initial In–Sb with a variable In/Sb ratio is used.

1. Introduction

The semiconducting properties of InSb are very well known [1–3]. Under certain circumstances (mainly applied pressure and temperature), the compound InSb may also become superconducting [4–6]. However, to our knowledge, the conversion of stoichiometric InSb into cermet compact acquiring special electrical resistivity characteristics has not yet been reported.

Generally, each cermet system consists of two main components, i.e. ceramics and metal [7]. The particular properties of cermets are utilized preferably in two areas of practical applications: first, as refractories possessing outstanding high-temperature strength and significant hardness, and second, as resistors having a low value of temperature coefficient of

electrical resistance [8].

This paper reports a study of a phase transformation of stoichiometric polycrystalline semiconducting InSb and InSb(La) into cermet InSb–Sb–In₂O₃ compact. The electrophysical characteristics of this compact and the synthesis and thermodynamic conditions of the transformation and conversion were investigated. The conversion of initial InSb and InSb(La) was performed by partial oxidation at elevated temperatures. It is demonstrated that the produced cermet compact exhibits rather unusual resistance behaviour and a small variation in electrical resistivity over a wide temperature range between 4 and 400 K. The initial InSb and InSb(La) were prepared by the rapid quenching method.

2. Experimental procedure

2.1. Preparation of the initial polycrystalline InSb and InSb(La)

The rapid quenching method was described in detail elsewhere [9]. Both types of material were produced in the form of short tapes 30–40 mm long, 3–6 mm wide and 50 μm thick. It was demonstrated previously [10], that the temperature dependence of the magnetoresistance coefficient $\Delta R/R_0 = f(T)$ of stoichiometric polycrystalline InSb is lowered in the temperature interval 20–100 $^{\circ}\text{C}$, when 1 mass % La_2O_3 is added to this compound, Fig. 1. Both, InSb and InSb(La) were therefore used as starting materials for our present studies.

2.2. InSb, InSb(La) samples and their processing

Because both the starting materials are very brittle, their manipulation was rather difficult. They were

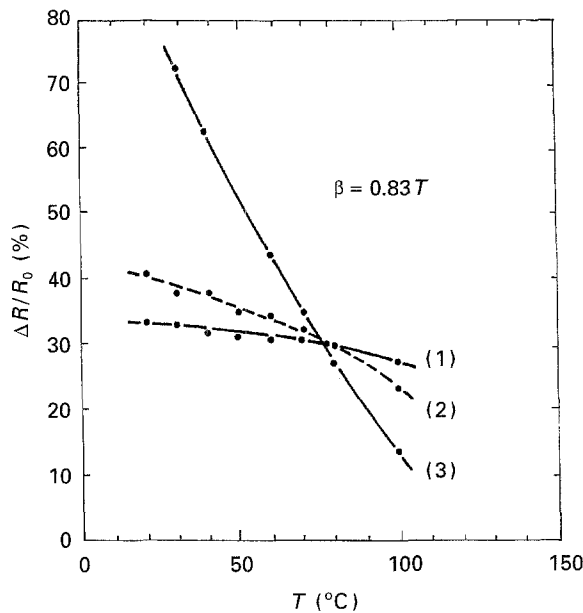


Figure 1 Magnetoresistance of InSb. (1) polycrystalline InSb(La), (2) polycrystalline InSb, both prepared by rapid quenching, (3) monocrystalline InSb.

therefore crushed in an agate mortar to a fine powder and pressed into compact pellets, 12 mm diameter and 1 mm thick. These pellets were then subjected to annealing in flowing oxygen under conditions close to those used previously for the preparation of HT_c superconductors [11]. In the present case a temperature interval from 200–500 $^{\circ}\text{C}$ was used for annealing (melting point of InSb is 525 $^{\circ}\text{C}$). The annealing time was 1–50 h. One InSb(La) sample was annealed for 50 h at 400 $^{\circ}\text{C}$ also in the original tape (uncrushed) form. A list of prepared pellet samples and their processing conditions is given in Table I.

2.3. Characterization of the samples

The electrical resistance of all the prepared samples was measured by the usual four-point d.c. method in the temperature range 4–400 K. Phase composition was examined by X-ray powder diffraction (XRPD) analysis with CuK_α radiation. From these results, the conversion degree, β (mass ratio of converted InSb or InSb(La) portion to the initial one), was evaluated and the magnitude of, f (the molar ratio of $\text{In}_2\text{O}_3/2\text{Sb}$) was calculated.

Because the oxidation of the semiconducting InSb was expected to be a process connected with weight changes and thermal effects, the thermogravimetric (TG) and differential thermogravimetric (DTG) measurements and differential thermal analysis (DTA) studies were performed on a Derivatograph analyser in air and flowing oxygen. The TG measurements were accomplished under isothermal conditions or with a dynamic temperature increase from room temperature to 1000 $^{\circ}\text{C}$.

The surface and fracture microstructures of samples were examined by scanning electron microscopy (SEM).

3. Results and discussion

3.1. $R(T)$ characteristics

The data summarized in Table I demonstrate some properties of heterogeneous cermet compacts obtained by partial oxidation of the initial bulk InSb and InSb(La) samples in flowing oxygen at temperatures

TABLE I The studied samples and their processing conditions. Conversion degree, β , is the mass ratio of converted to initial InSb, f is the molar ratio $\text{In}_2\text{O}_3/2\text{Sb}$, z is the volatilized portion of Sb, f_{mr} is the relative mass change of the oxidized system (5)

Sample	Material annealed	Annealing conditions			Thermal parameters			
		Temp. ($^{\circ}\text{C}$)	Time (h)	Medium	β	f	z	f_{mr}
1.	InSb(La)	–	–	–	–	–	–	1
2.	InSb	–	–	–	–	–	–	1
3.	InSb(La)	200	50	O_2	0	–	–	1
4.	InSb(La)	250	50	O_2	0.132	0.500	–	1.002
5.	InSb(La)	275	50	O_2	0.186	0.500	–	1.019
6.	InSb(La)	300	50	O_2	0.282	0.500	–	1.029
7.	InSb(La)	400	1	O_2	0.359	0.500	–	1.036
8.	InSb(La)	400	10	O_2	0.741	0.645	0.450	0.989
9.	InSb(La)	400	25	O_2	0.781	0.705	0.582	0.962
10.	InSb(La)	400	50	O_2	0.836	0.950	0.947	0.881
11.	InSb	400	50	O_2	0.801	0.850	0.824	0.912
12.	InSb(La)	500	50	O_2	0.990	2.360	1.576	0.699

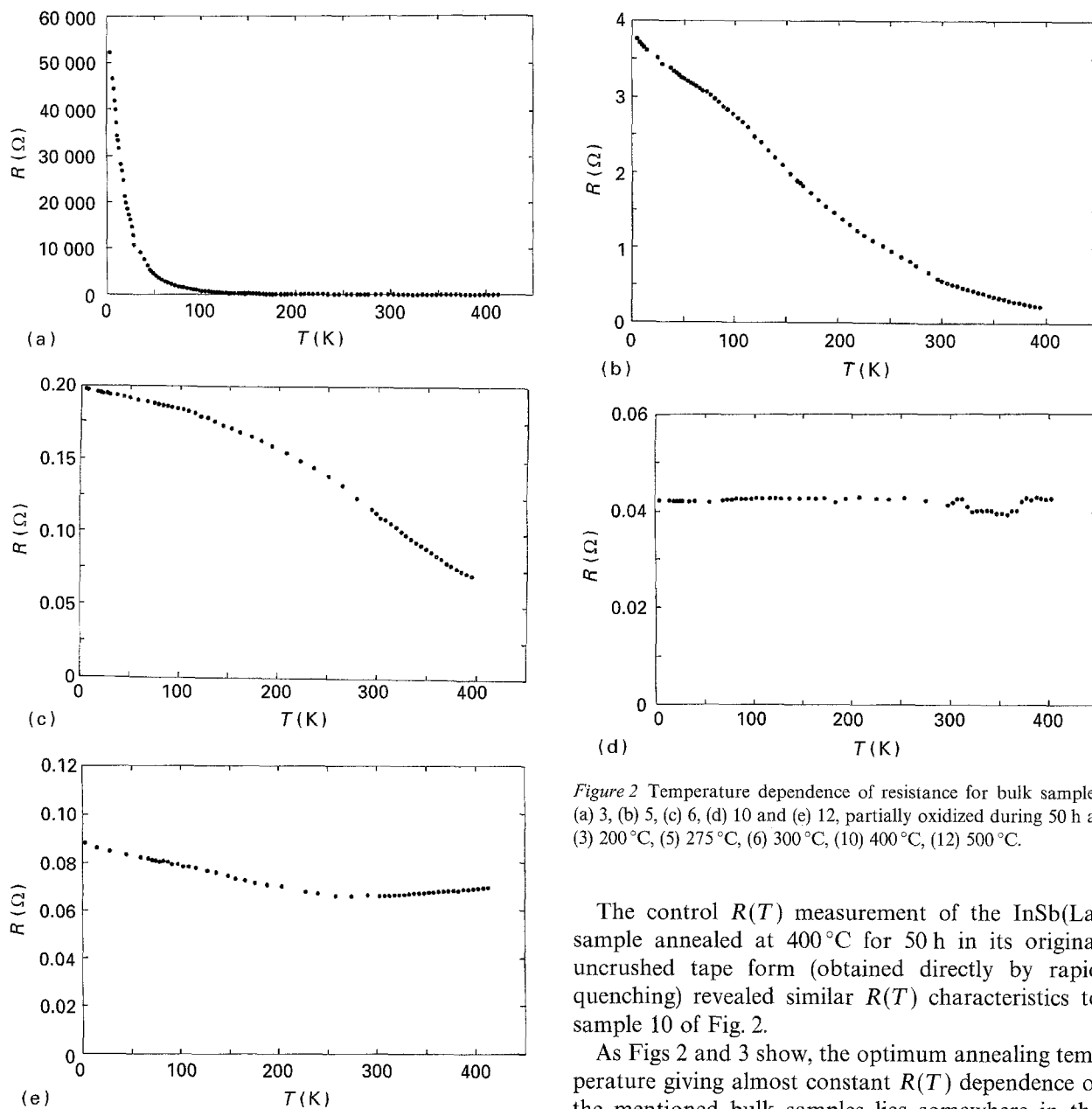


Figure 2 Temperature dependence of resistance for bulk samples (a) 3, (b) 5, (c) 6, (d) 10 and (e) 12, partially oxidized during 50 h at (3) 200 °C, (5) 275 °C, (6) 300 °C, (10) 400 °C, (12) 500 °C.

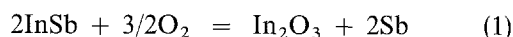
The control $R(T)$ measurement of the InSb(La) sample annealed at 400 °C for 50 h in its original uncrushed tape form (obtained directly by rapid quenching) revealed similar $R(T)$ characteristics to sample 10 of Fig. 2.

As Figs 2 and 3 show, the optimum annealing temperature giving almost constant $R(T)$ dependence of the mentioned bulk samples lies somewhere in the vicinity of 400 °C. It was therefore decided to process a thin layer of initial stoichiometric InSb material in a similar way. A thin film 1 μm thick was prepared on single-crystalline MgO substrate by evaporation of polycrystalline InSb. Such a sample was then partially oxidized at 400 °C for 50 h. The $R(T)$ dependence measured in the temperature range from 4.2 K (boiling liquid helium) to 300 K (room temperature) for this film is plotted in Fig. 4.

3.2. Results of XRPD analysis and SEM observations

It was established that the $R(T)$ dependences of partially oxidized bulk samples of InSb and InSb(La) depend on annealing conditions (time, temperature, atmosphere) and thus, on the phase composition of the ternary InSb–Sb–In₂O₃ system and the conversion degree, β , according to Reaction 1. Some selected physical and crystallographic properties of the individual components InSb, In, Sb, In₂O₃, Sb₂O₃, Sb₂O₄, related to the synthesis and oxidation of the InSb system are collected in Table II.

under 400 °C when no element is escaping from the system according to the reaction



Products of the oxidizing process are the semiconducting In₂O₃ and metallic antimony, the rest being the unconverted InSb or InSb(La).

The temperature dependence of electrical resistance, $R(T)$, for samples 3, 5, 6, 10 and 12 of Table I, all annealed for 50 h, is illustrated in Fig. 2 for the temperature range 4–400 K. It was found that the La₂O₃ addition influences the $R(T)$ dependence only slightly. An important discovery was the existence of relatively constant electrical resistance over a rather wide temperature range from 4–400 K. This state was achieved after isothermal heating at 400 °C. The $R(T)$ dependence for samples annealed at 400 °C for 50 h, Fig. 2, and 1 h, Fig. 3, showed a similar character, exhibiting a rather uniform resistivity. The samples annealed at lower (200, 275, 300 °C) or higher (500 °C) temperatures exhibited a semiconductive character, Fig. 2.

The selected angular intervals of the XRPD patterns ($\theta = 11^\circ\text{--}17^\circ$) of unreacted InSb(La) (sample 1 of Table II) and samples annealed in an oxygen atmosphere for 50 h at 250 °C (4), 300 °C (6), 400 °C (10), and 500 °C (12) are shown in Fig. 5. The XRPD patterns of samples annealed at 400 °C in oxygen for 1 h (7), 10 h (8), 25 h (9) and 50 h (10) are plotted in Fig. 6.

The XRPD data were used for evaluation of the β quotients of Reaction 1 and the f values for each oxidized InSb sample. The calculated β values are

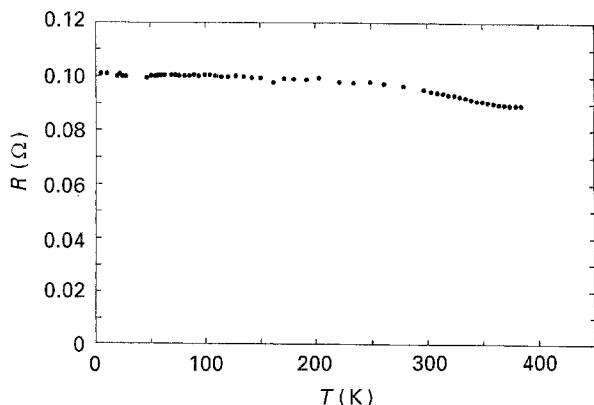


Figure 3 Temperature dependence of electrical resistance for bulk sample 7 of Table I partially oxidized at 400 °C for 1 h.

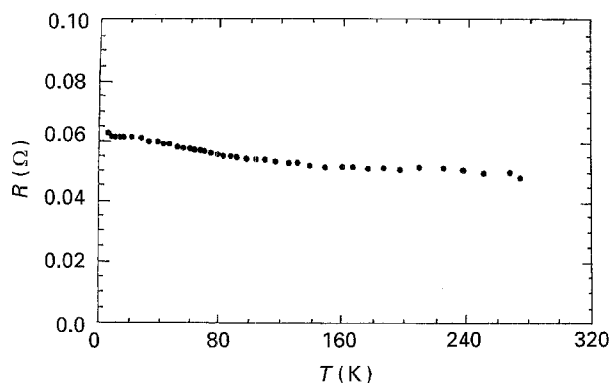


Figure 4 Temperature dependence of electrical resistance of a thin film 1 μm thick partially oxidized at 400 °C for 50 h.

summarized in Table I. According to this table, β increases with increasing temperature and annealing time.

The f value, 0.5, should remain independent of reaction time and temperature, as long as Reaction 1 is the only reaction in the high-temperature process. However, a change in f becomes evident (i.e. $f > 0.5$), when the annealing process occurs in an oxygen atmosphere at temperatures higher than 400 °C, or when the reaction time exceeds some threshold value (samples 8–12, Table I). Thus metallic antimony is escaping partially from the system either in an elemental form (Sb) or in an oxidized form (Sb_2O_3 or Sb_2O_4) or by evaporation in both forms. Therefore, because of this, only integral X-ray intensities of the In_2O_3 and InSb phases can be used for evaluation of the conversion degree, β . Additional information concerning the oxidation process of InSb could be derived from the thermogravimetric measurements.

The development of microstructure in the InSb–Sb– In_2O_3 compact throughout the isothermal annealing at 400 °C is well recognized from the records taken on the samples after 1 and 50 h annealing by SEM. A gradual grain growth with increasing annealing time was recognized. Apparently, the gradually lowered extent of grain boundaries with

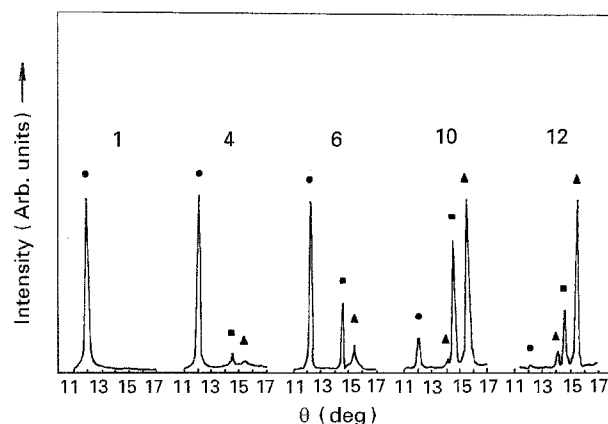


Figure 5 XRPD patterns for selected interval of $\theta = 11^\circ\text{--}17^\circ$: (1) initial material, bulk samples annealed 50 h; (4) 250 °C; (6) 300 °C; (10) 400 °C; (12) 500 °C. (●) InSb, (■) Sb, (▲) In_2O_3 .

TABLE II Some selected physical and crystallographic properties of InSb, In, Sb, In_2O_3 , Sb_2O_3 and Sb_2O_4

	InSb	In	Sb	In_2O_3	Sb_2O_3	Sb_2O_4
Electrical properties	Semiconductor	Metal	Metal	Semiconductor	Insulator	Insulator
Habit (appearance)	Dark metallic	Silver-like white metal	Silver-like white metal	Light-yellow powder	White–grey powder	White–grey powder
Melting point (°C)	525	156.4	630.5	850, volatilizes	656	930, decomposes
Boiling point (°C)	–	2000	1380	–	1550, sublimes	–
Symmetry	Cubic	Tetragonal	Rhombohedral	Cubic	Cubic	Cubic
Type of structure	Sphalerite	$\gamma\text{-Mn}$	–	Bixbyite	–	$\text{Sb}^{\text{III}}\text{Sb}^{\text{V}}\text{O}_4$
Space group	$F\bar{4}3m$	$14/mmm$	$R\bar{3}m$	12_13	$Fd\bar{3}m$	$Fd\bar{3}m$
Unit cell: a (nm)	0.648 41	0.325 20	0.450 65	1.011 8	1.115 2	1.028 0
b (nm)	0.648 41	0.325 20	0.450 65	1.011 8	1.115 2	1.028 0
c (nm)	0.648 41	0.494 70	0.450 65	1.011 8	1.115 2	1.028 1
α, β, γ (deg)	90,90,90	90,90,90	57.1;57.1;57.1	90,90,90	90,90,90	90,90,90
Unit cell volume (nm^3)	0.272 62	0.051 965	0.060 401	1.035 82	1.386 94	1.086 37
Theoretical density, D_x (kg m^{-3})	5763	7337	6693	7117	5583	7519
Number of formula units, Z , in the unit cell	4	2	2	16	16	16

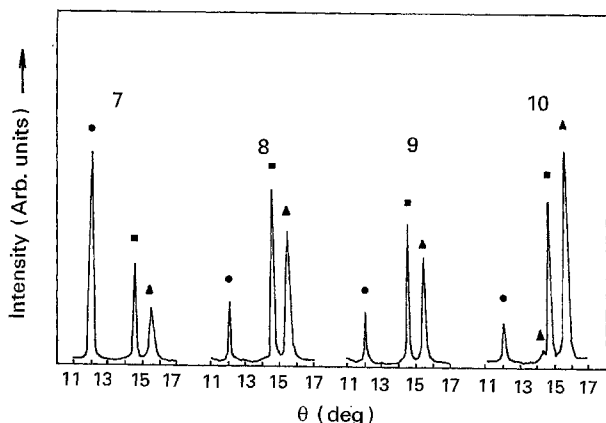


Figure 6 XRPD patterns for $\theta = 11^\circ\text{--}17^\circ$. Bulk samples annealed at 400°C : (7) 1 h, (8) 10 h, (9) 25 h, (10) 50 h. (●) InSb, (■) Sb, (▲) In_2O_3 .

annealing time, as well as the presence of metallic antimony, are both responsible for the lower resistance of these samples.

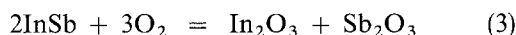
3.3. Thermochemical studies

Reaction 1 is a heterogeneous-type process, in which solid-state disintegration of InSb and oxidation of indium by gaseous oxygen take place. Reaction 1 is one of several other possible parallel reaction paths, which has the lowest energy barrier and the fastest path and a dominating contribution to the overall process at temperatures under 400°C . However, the reaction rate constant, K_r , is dependent on the annealing temperature, T , according to the relation

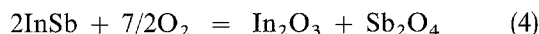
$$K_r = \frac{kT}{h} \exp\left(-\frac{\Delta H^*}{RT}\right) \exp\left(\frac{\Delta S^*}{R}\right) \quad (2)$$

where k is the Boltzmann constant, h is the Planck constant, and ΔH^* , ΔS^* are the enthalpy and entropy of activation, respectively.

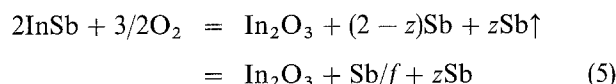
At temperatures equal to or higher than 400°C , other oxidation reactions may take place, e.g.



or [12]



owing to the shift of the reaction-rate constant value in favour of Reactions 3 and 4. A reaction connected with formation of metallic Sb and partial escape of $\text{Sb}\uparrow$ from the system can be also considered:



where z is the volatilized portion of Sb and f is the molar ratio of the reaction products i.e. $f = \text{In}_2\text{O}_3/(2-z)\text{Sb} = 1/(2-z)$. Obviously, according to the temperature level and reaction time, all five phases i.e. InSb, Sb, In_2O_3 , Sb_2O_3 and Sb_2O_4 , can constitute the reaction product. At the same time, oxidation conversion of InSb into ternary, quaternary or quinary phase assemblages increases the phase-boundary interface, thus imposing new limita-

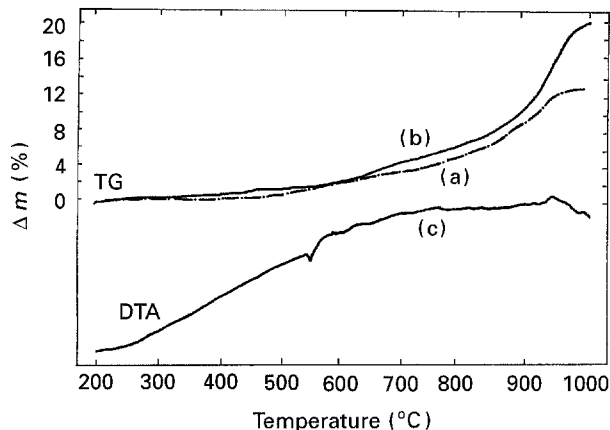


Figure 7 Thermochemical data for the InSb-Sb- In_2O_3 system synthesized according to Reaction 1: (a) TG data, annealing in air, 9°C min^{-1} ; (b) TG data, annealing in oxygen, 5°C min^{-1} ; (c) DTA data, annealing in oxygen, 5°C min^{-1} .

tions upon the overall reaction rate. It is well known, that the rate-determining processes are: material transport to the interface, reactions at the interface boundary, transport of reaction products away from the interface, and absorption or liberation of the reaction heat. Any of these processes may determine the overall reaction rate in our case.

The calculated relative mass increase for Reaction 1 is 10.1%, for Reaction 3 is 20.3%, and for Reaction 4 is 23.7%. Fig. 7, shows the mass increase in the system InSb- $\text{O}_2(\text{N}_2)$ (flowing air) under dynamic heating conditions (9°C min^{-1}) from room temperature to 1000°C . The TG curve shows no significant angular bending in the mass increase as a function of temperature, nor a delayed course which would indicate a new reaction step. This would mean, that all oxidation conversion processes of indium and antimony into In_2O_3 , Sb_2O_3 and Sb_2O_4 may generally overlap. The mass increase of the heated system begins at around 400°C . The oxidation process becomes more intense at temperatures above the melting point of InSb (525°C), as well as above the melting points of antimony (630.5°C) and Sb_2O_3 (656°C). The melting point of Sb_2O_4 at 930°C is connected with a loss of oxygen. The total mass increase of the whole system by heating in air up to 1000°C was found as 18.3 mass %, which is less than the expected increase according to Equation 4, i.e. 23.7%. This confirms a partial escape of antimony from the system, as was indicated by the XRPD analysis.

The dynamic heating of InSb in flowing oxygen at the rate of 5°C min^{-1} , Fig. 7, indicates that a mass increase has already occurred at temperatures above 250°C . The further mass increase has a similar character to the heating curve for InSb from TG measurements in air. The total mass increase of the oxidized system was found to be 19 mass %. Thus, the partial escape of antimony from the system also takes place in the oxygen atmosphere.

The only significant endothermic effect on the DTA trace of Fig. 7c, performed with a 5°C min^{-1} heating rate in an oxygen atmosphere belongs to the melting process of InSb at 525°C . In the remaining part of the DTA record, a broad compensation of exothermic

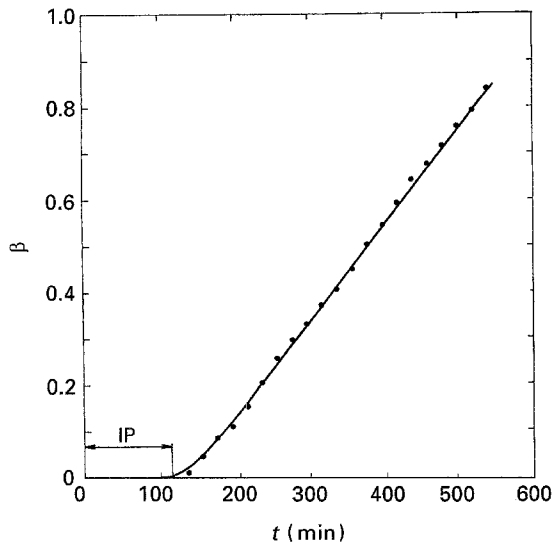


Figure 8 Dependence of conversion degree, β , on the time of isothermal heating (425 °C) in an oxygen atmosphere.

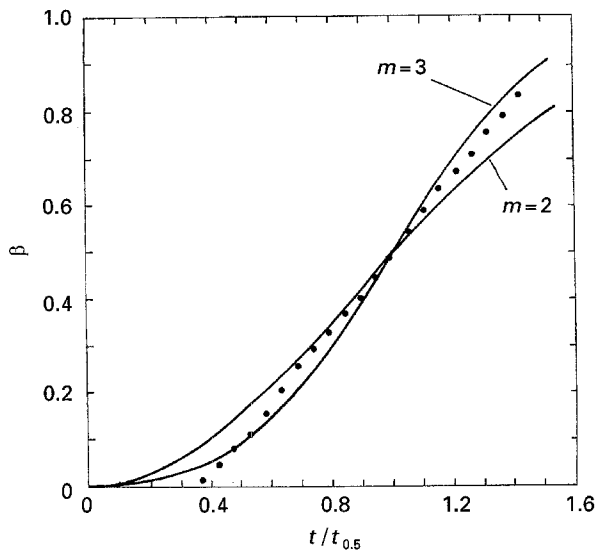


Figure 9 Dependence of β on the ratio $t/t_{0.5}$ in an oxygen atmosphere. The experimental points indicate concurrent two- and three-dimensional nucleation-growth mechanisms, Reaction 5.

(oxidation) and endothermic (melting, evaporation) effects, exists.

The isothermal TG measurement of the In-Sb-O system was limited to such an ambient atmosphere and range of temperatures, at which the only dominant process was the partial oxidation (Reaction 1) with a sufficiently high reaction rate. Reactions 3 and 4 actually represent consecutive reaction steps which also include that expressed by Reaction 1. All these reactions, together with an eventual additional escape of antimony from the system, make interpretation of the obtained experimental results rather confusing.

Fig. 8 represents the dependence of the conversion degree, β , on the annealing time, t . A long induction period (IP) may be noticeable ($IP > 100$ min). The relative mass change of the oxidized system (5), f_{mr} , is given as:

$$\begin{aligned} f_{mr} &= [2(1 - \beta)M_{InSb} + \beta M_{In_2O_3} \\ &\quad + (2 - z)\beta M_{Sb}]/2M_{InSb} \\ &= 1 + 0.1014\beta - 0.2573\beta z \end{aligned} \quad (6)$$

where M_x represents the corresponding molecular weight of the constituent x (InSb, In_2O_3 or Sb).

As a probable mechanism for Reaction 1, Fig. 9 indicates a nucleation-growth process. In Fig. 9, the ratio $t/t_{0.5}$ represents the normalized reaction time, $t_{0.5}$ is the half-time of the reaction, when 50% of InSb is converted into reaction product. The real nucleation-growth mechanism is described by a combined Johnson-Mehl-Avrami-Jerofyejev-Kolgomorov (JMAJK), equation [13]

$$-\ln(1 - \beta) = ct^m \quad (7)$$

where β is the conversion degree, and c is the total rate constant of Reaction 1. The value of exponent m depends on the dimensionality (one-, two- or three-dimensional process) and also on the rate-controlling processes (chemical reaction, diffusion). It can also acquire non-integer values.

The $\beta = f(t/t_{0.5})$ analysis shows that the reaction mechanism is of a nucleation-growth type and its m value lies between 2 and 3. Curves for $m = 2$ and 3 of Fig. 9 represent the model curves for two- and three-dimensional processes. It indicates that the dimensionality of the nucleation-growth process lies between two-dimensional and three-dimensional geometry and, that both oxidation and diffusion processes probably take part in particle growth. The relaxation of the nucleation process can be expressed through a multiplication of the $-\ln(1 - \beta)$ term in Equation 5 by a modulating term.

4. Conclusion

Phase transformation of stoichiometric semiconducting InSb and InSb(La) into InSb-Sb- In_2O_3 cermet compact (InSb, In_2O_3 -semiconductors, antimony-metallic conductivity), having a relatively constant electrical resistance over a wide temperature interval, was achieved. Electrophysical properties and thermochemical processes were studied and measured for samples prepared mainly in the bulk form. The processing of the studied samples was performed in an oxidizing atmosphere at elevated temperatures (200–500 °C) for 1–50 h.

It was established that the resistance of the samples and its temperature dependence, $R(T)$, in the 4–400 K temperature range, is strongly influenced by annealing conditions (temperature, time and surrounding atmosphere) and thus also the degree of conversion, β . A relatively constant electrical resistance value was found over the whole measuring interval (4–400 K) for samples annealed at 400 °C. Similar behaviour was also found in the case of thin 1 μ m thick InSb film processed under the same annealing and oxidizing conditions as bulk samples.

From the XRPD patterns and observations, the conversion degree, β (mass ratio of converted to unconverted portion of InSb), and the f value (molar ratio of In_2O_3 to 2Sb in the reaction $2InSb + 3/2 O_2 = In_2O_3 + 2Sb$), were calculated. β was found to increase with increasing temperature and time of

annealing. However, instead of being independent of reaction temperature and time, the expected $f = 0.5$ value increases for oxidizing temperatures higher than 400 °C and for oxidizing annealing times longer than 1 h. This was due to the partial escape of metallic antimony from the InSb–Sb–In₂O₃ system either in an elementary form as Sb, or in an oxidized form as Sb₂O₃ or Sb₂O₄, or in both forms. Additional information concerning the oxidation processes in InSb or InSb(La) during oxidizing annealing was therefore required, and was derived from thermogravimetric measurements. The SEM observations showed an increasing grain size of converted cermet compact with temperature and time of oxidizing annealing, thus lowering the density of grain boundaries and accordingly (together with developing portion of metallic antimony component) also the electrical resistance.

The TG and DTG measurements and DTA studies revealed that the nucleation and growth of the reaction products, i.e. In₂O₃ and antimony in the InSb–Sb–In₂O₃ compact, leads to a conduction process, in which metallic nuclei with a positive temperature coefficient of electrical resistance are separated by semiconducting In₂O₃ and InSb matrices with negative temperature coefficients of resistance. The metallic particles embedded in a semiconductive matrix form percolative paths, in which the tunnelling process is almost temperature independent, because the semiconductive character of In₂O₃ and InSb may reduce the metallic–conductive character of antimony and its positive temperature coefficient to almost zero.

It was supposed that an addition of 1 mass % La₂O₃ to the initial stoichiometric InSb would lower the thermal coefficient of electrical resistance but it was found that its influence upon the electrophysical properties of the studied samples was rather low or

even negligible. On the other hand, it is believed that the transformation reactions, as well as the properties of the prepared new material, might be influenced significantly if, instead of stoichiometric InSb as an initial material, In–Sb with variable In/Sb ratio, was used.

References

1. M. RODOT, "Les matériaux semi-conducteurs" (Dunod, Paris, 1965) in Russian (Moscow, 1971) pp. 150, 158.
2. H. WEISS, "Physik und Anwendung galvanomagnetischer Bauelemente" (Vieweg, Braunschweig, 1969) p. 57.
3. H. H. WIEDER, "Intermetallic semiconducting films" (Pergamon Press, Braunschweig, 1970) pp. 85, 122, 216.
4. D. B. McWHAN and M. MAREZIO, *J. Chem. Phys.* **45** (1966) 2508.
5. S. MINOMURA, B. OKAI, Y. ONODA and S. TANUMA, *Phys. Lett.* **23** (1966) 641.
6. M. D. BANUS and M. C. LAVINE, *J. Appl. Phys.* **38** (1967) 2042.
7. W. D. KINGERY, H. K. BOWEN and D. R. UHLMANN, "Introduction to Ceramics" (Wiley, Chichester, 1976) pp. 498, 573.
8. J. GASPERIČ, PhD thesis, University of Ljubljana (1972) p. 53.
9. J. ČERVENÁK and P. DUHAJ, "Equipment and procedure for preparation of polycrystalline semiconductors" (in Slovak), former Czechoslovakia Pat. 251544, 13 November 1986.
10. J. ČERVENÁK, Internal report IEE SAS, Bratislava (1989).
11. M. JERGEL, F. HANIC, V. ŠTRBÍK, J. LIDAY, G. PLESCH, T. MELÍŠEK and M. KUBRANOVÁ, *Supercond. Sci. Technol.* **5** (1992) 663.
12. P. S. GOPALAKRISHNAN and H. MANOHAR, *J. Solid State Chem.* **16** (1976) 301.
13. J. ŠESTÁK, "Measurement of thermophysical properties of solid materials. Theoretical thermal analysis" (in Czech) (Academia Press, Prague, 1982) p. 153.

Received 15 February
and accepted 8 September 1994